Canadian Science Publishing

ARTICLE

Physical modelling of pile drilling in sand

Einar John Lande, Stefan Ritter, Henning Tyvold, and Steinar Nordal

Abstract: Drilling for foundation piles and tieback anchors through soils using a continuous casing to support the borehole is often referred to as "overburden drilling". Monitoring data from several case studies show that overburden drilling may cause considerable short-term ground settlements indicating a loss of soil volume around the casings. However, further insight is required to understand the mechanisms that govern overburden drilling. Novel physical model tests were carried out to investigate the effects of varying parameters such as flushing media (water or air), flow and penetration rate on the penetration force, pore pressure changes, soil displacements, and drill cutting transport. Tests with water flushing indicate a clear relation between the flow and penetration rate and the resulting influence on the surrounding ground. Increasing flow rates caused larger excess pore pressures at greater radial distances and generated more excess drill cuttings compared to the theoretical casing volume. The obtained results were translated into a non-dimensional framework to estimate optimal flushing parameters in similar conditions. The air flushing tests were considerably limited by the modelling constraints. Notable reduction of pore pressures adjacent to the casing indicate an air-lift pump effect that can lead to extensive ground movements as observed in the field.

Key words: model tests, drilling, piles, anchors, settlement, pore pressure.

Résumé : Le forage de pieux de fondation et d'ancrages d'arrimage dans le sol à l'aide d'un tubage continu pour soutenir le trou de forage est souvent appelé « forage dans les morts-terrains ». Les données de surveillance provenant de plusieurs études de cas montrent que le forage de morts-terrains peut provoquer des tassements considérables du sol à court terme, indiquant une perte de volume de sol autour des tubages. Toutefois, il est nécessaire de mieux comprendre les mécanismes qui régissent le forage des morts-terrains. De nouveaux essais sur modèle physique ont été réalisés pour étudier les effets de divers paramètres tels que le milieu de rinçage (eau ou air), le débit et le taux de pénétration sur la force de pénétration, les changements de pression interstitielle, les déplacements de sol et le transport des déblais de forage. Les essais avec rinçage à l'eau indiquent une relation claire entre le débit et le taux de pénétration et l'influence conséquente sur le sol environnant. L'augmentation des débits a entraîné des pressions de pores plus importantes à des distances radiales plus grandes et a généré plus de déblais de forage en excès par rapport au volume théorique du tubage. Les résultats obtenus ont été traduits dans un cadre non dimensionnel pour estimer les paramètres de rinçage optimaux dans des conditions similaires. Les essais de chasse d'air ont été considérablement limités par les contraintes de modélisation. Une réduction notable de la pression des pores adjacents au tubage indique un effet de pompe à air qui peut entraîner des mouvements importants du sol, comme on l'a observé sur le terrain. [Traduit par la Rédaction]

Mots-clés : essais sur maquettes, forage, pieux, ancrages, tassement, pression interstitielle.

1. Introduction

In areas where soft soil deposits of limited depth are overlying competent bedrock so-called overburden drilling is often carried out to install tieback anchors for sheet pile walls (SPWs) as well as end bearing foundation piles into bedrock. Overburden drilling is characterized by permanent casings that are penetrated through the soil (i.e., overburden) using rotary percussive drilling until it reaches bedrock (Sabatini et al. 2005; Finnish Road Authorities 2003). Recent case histories reported by Langford et al. (2015) indicate that overburden drilling for tieback anchors and piles from inside deep excavations in soft clay may cause ground settlements that exceed those reported in previous studies, e.g., Peck (1969), Mana and Clough (1981), Karlsrud and Andresen (2008). While previous research extensively studied the effects from displacements of the retaining walls as well as consolidation effects, few studies have investigated the mechanisms of overburden drilling. Understanding the installation effects and influence from overburden drilling on the surrounding ground is vital to avoid damages on adjacent buildings.

Reported field tests (Lande et al. 2020; Ahlund and Ögren 2016) and case records (Konstantakos et al. 2004; Kullingsjø 2007; Bredenberg et al. 2014; Sandene et al. 2021) indicate that overburden drilling with air driven down-the-hole (DTH) hammers may cause significant excess ground settlements immediately after drilling. These findings are likely explained by a loss of soil

Received 18 June 2020. Accepted 2 November 2020.

E.J. Lande. Department of Sustainable GeoSolutions, Norwegian Geotechnical Institute, P.O. Box 3930, Oslo N-0806, Norway; Department of Civil and Environmental Engineering, Norwegian University of Science and Technology (NTNU), Trondheim 7491, Norway.
S. Ritter. Department of Onshore Foundations, Norwegian Geotechnical Institute (NGI), Oslo, Norway.
H. Tyvold and S. Nordal. Department of Civil and Environmental Engineering, Norwegian University of Science and Technology (NTNU), Trondheim 7491, Norway.

Corresponding author: Einar John Lande (email: einar.john.lande@ngi.no).

Fig. 1. Test set-up: (*a*) model tank and (*b*) flushing pressure line. (1 bar = 100 kPa.) [Colour online.]

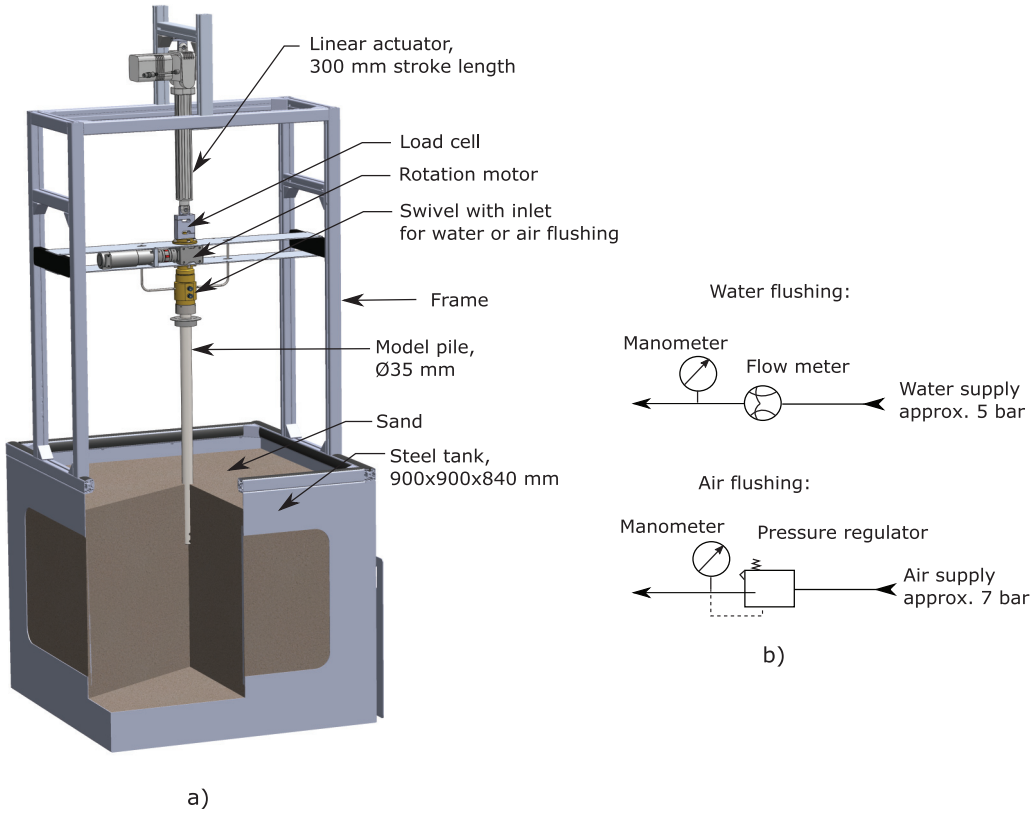

volume around the casings that was often observed when drilling through silty and sandy soils, or granular material (i.e., a moraine layer) above bedrock. The soil loss might be related to the so-called air-lift pump effect (Behringer 1930; Kato et al. 1975) as silt and sand particles are eroded and transported to the ground surface. By contrast, the studies reported by Lande et al. (2020), Asplind (2017), and Ahlund and Ögren (2016) indicate that drilling with a water driven DTH hammer caused less settlements and excess pore pressures compared to air flushing. None of the previous studies included systematic and accurate measurements of drill cutting volume or mass to assess the potential soil volume loss and to verify the hypothesis of the air-lift pump effect. Neither have systematic studies of the effects of drilling parameters on the soil response to overburden drilling including pore pressure changes and soil displacements been carried out.

Another mechanism that was observed with overburden drilling is uncontrolled piping or hydraulic fracturing (i.e., pneumatic blowouts) along the outside of the casing, which was predominantly identified when flushing with compressed air (Lande et al. 2020; Sandene et al. 2021). This behaviour typically occurs during drilling of the first metres below ground surface due to low soil stresses, but it has also been observed when drilling at large depths (e.g., depths >20 m). Such piping effects are comparable to fluidization that has been investigated extensively (Tsinker 1988; van Zyl et al. 2013; Alsaydalani and Clayton 2014; de Brum Passini and Schnaid 2015).

There has been limited research on installation effects of overburden drilling, hence the mechanisms affecting the surrounding ground are not fully understood. In this context, a physical modelling approach was chosen. A series of pile drilling tests in saturated sand was carried out at the Norwegian Geotechnical Institute (NGI) in Oslo, Norway. The objective was to deepen the understanding of the mechanisms due to flushing with water or air and to investigate how the drilling parameters penetration and flushing rate affect the influence on the surrounding soil. The present research aims at providing knowledge that can be used in planning and execution of overburden drilling to reduce the risk of unwanted influence on the surrounding ground. The following section gives a detailed description of the experimental set-up including the model tank and the model pile, instrumentation, drilling simulation, and test procedure. After the results are presented and discussed, conclusions are drawn.

2. Experimental set-up

A novel test set-up made it possible to replicate overburden drilling using a small-scale pile (i.e., casing with an internal drill string and drill bit) with simultaneous penetration, rotation, and water or air flushing to transport the drill cuttings.

2.1. Model tank and instrumentation

Figure 1 illustrates the model test set-up. The soil model was placed in a cube shaped steel tank (Fig. 1*a*). An aluminium reaction frame was fixed to the top of the model tank, acting as support for a linear actuator used to vertically move the pile. The actuator had a maximum stroke length of 300 mm and a push capacity of 8000 N. A load cell with a capacity of 5000 N was connected between the actuator and a rotation motor unit to measure the penetration force on the pile during the tests. The rotation motor had a swivel unit that made it possible to flush with water or air through the pile drill string and drill bit at the same time as the entire pile rotated and penetrated. Both the penetration rate and rotation speed (rpm) of the pile were controlled by adjusting the voltage on the respective power supplies. The pile penetration was measured with an extensometer connected to the frame and rotation motor.

Figure 1*b* shows a schematic illustration of the pressure lines for both water and air flushing. The water supply came directly from the main supply tap with an approximate pressure of

Fig. 2. Experimental setup: (*a*) plan view, (*b*) cross section A-A through pore-water pressure sensors (PPs), and (*c*) cross section B-B through linear variable differential transformers (LVDTs). (All dimensions in millimetres.)

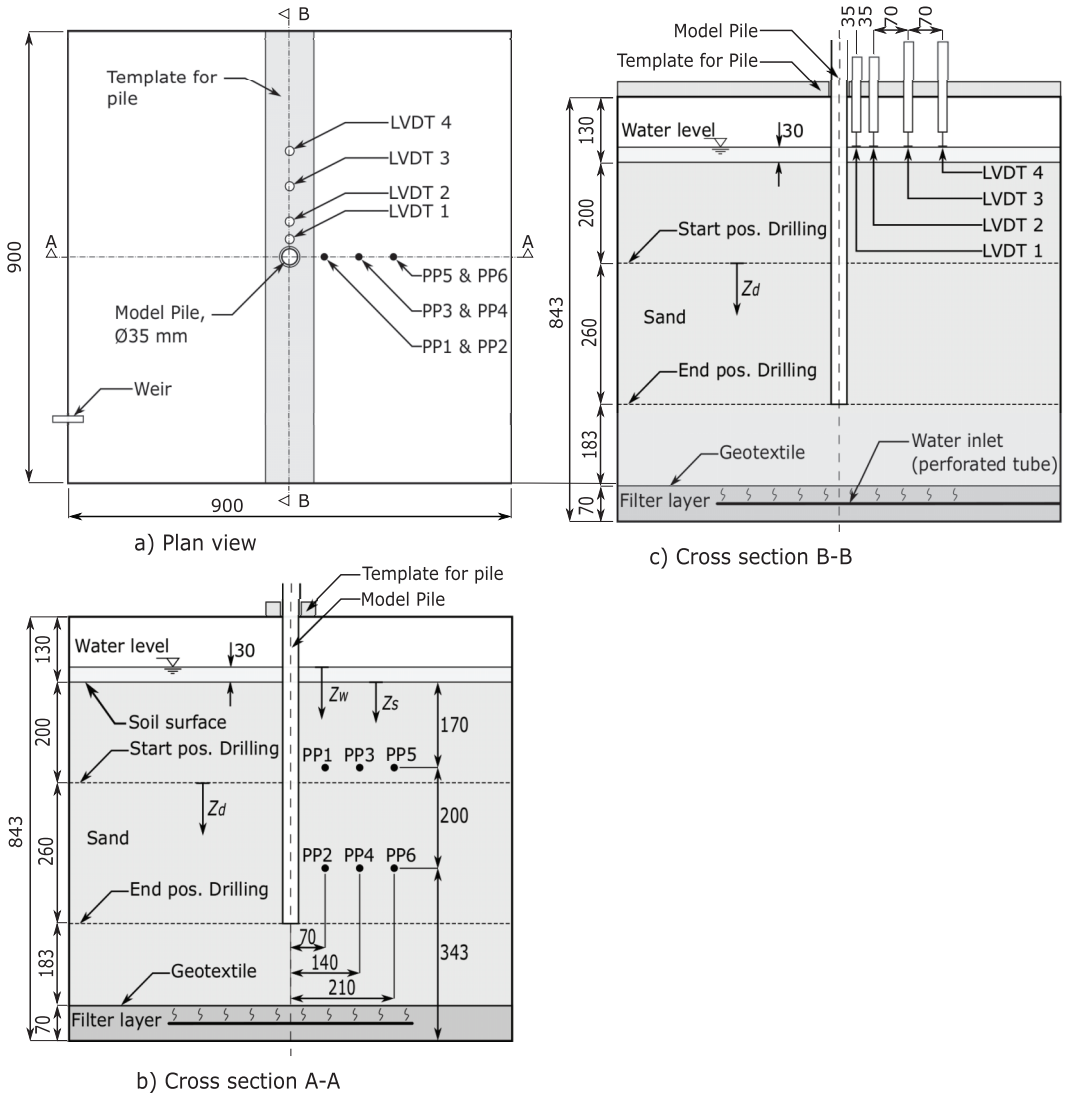

500 kPa. A flow meter was used to control the flow rate while a manometer was used to monitor the water pressure delivered to the pile during a test. For the air flushing tests, a pressure regulator with a manometer was used to control the pressure from the supply that had a pressure of approximately 700 kPa.

The entire tests were carried out with the model pile placed in the centre position of the soil model. Figure 2 presents a layout (Fig. 2*a*) and cross sections (Figs. 2*b* and 2*c*) of the model test set-up including the instrumentation used to monitor the soil response. Measurements of pore-water pressures in the sand model were obtained using standpipes, i.e., plastic tubes with a diameter of 4 mm, that were connected to pressure sensors located at the outside of the model tank. Six standpipes were installed at two different soil depths (Z_s = 170 and 370 mm) and with three radial distances from the pile centre (r = 70, 140, and 210 mm) as can be seen in Fig. 2*b*. The standpipes were supported and kept at the correct positions in the sand model throughout the entire test program by fastening them to three vertical steel rods (Ø10 mm) that were connected to a steel plate placed on the bottom of the model tank (see illustration in Section 2.3). A filter was placed at the top of each standpipe to prevent sand grains from entering and affecting the measurements. All sensors were calibrated before the conducted test series, and the values checked before each test to verify that the standpipes were unaffected.

Vertical displacements of the soil surface (i.e., settlements) were measured with four linear variable differential transformers (LVDTs) positioned at different distance from the pile (Figs. 2*a* and 2*c*). A gantry (template for pile in Fig. 2*c*) was used to keep the pile and the LVDTs in position during the tests.

2.2. Model pile and drilling simulation

Figure 3 shows a drawing of the model pile including details of the drill bit. The model pile is 890 mm long and consist of a casing, i.e., a steel tube with an outer diameter of 35 mm and thickness of 2 mm as can be seen in Fig. 3*a*. The flushing medium (water or air) is applied from the swivel device on the top of the pile through an inner steel tube with internal diameter of 6 mm. Between the casing and the inner tube is a middle steel tube that creates an annulus against the outer casing. The flushing backflow is transported through this annulus to the top of the pile, where a small catch-pot is used to collect the backflow (water and soil).

A drill bit is connected to the bottom of the casing–pile with six bolts. Four openings with a diameter of 4 mm were drilled

Fig. 3. Model pile: (*a*) cross section and (*b*) inner parts excluding casing. [Colour online.]

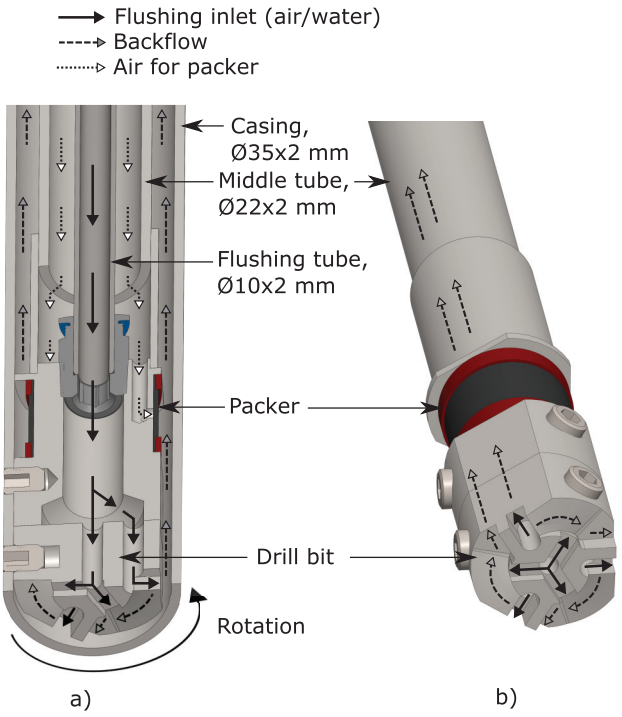

through the drill bit and are used as the flushing inlet during drilling (Fig. 3*b*). The face of the drill bit was designed with cutting grooves at each flushing inlet to direct the flushing media and drill cuttings towards the backflow paths like a typical prototype design. The upper part of the drill bit has a packer system that enables one to close the annulus between the casing and middle tube to collect the soil particles in this annulus at the end of each test. The packer consists of a rubber membrane fixed with tie wrap and can be activated by pumping air into it.

The pile diameter was adapted to the model tank to limit potential boundary effects. The mechanical design was based on a prototype concentric drill system named "Symmetrix" (Epiroc 2020) with a 114 mm diameter casing, resulting in a scale ratio of about 1:3.2 between the diameter of the model pile and the prototype. The dimensions (i.e., cross-sectional area) of the flushing tube and flushing inlet channels in the drill bit as well as the annulus for the backflow were all based on the prototype to obtain representative flushing conditions.

2.3. Sand model preparation

Figure 4 depicts different stages of the initial soil model preparation that was only carried out once for the entire test series. Two perforated plastic tubes were placed at the bottom of the model tank (Fig. 4*a*). One tube was used to pump water into the tank, i.e., applying an upward gradient, and the second tube for draining water from the bottom, i.e., applying a downward gradient. A permeable layer of approximately 70 mm lightweight expanded clay aggregates (LECA) was then placed over the perforated tubes (Fig. 4*b*). A geotextile layer was placed on top of the LECA and taped to the sides of the steel tank (Fig. 4*c*). The model tank was then filled with dry sand up to a thickness of about 640 mm (Fig. 4*d*).

All tests were carried out using Baskarp sand No. 15 (from Sibelco AB), which is a graded fine sand with well-documented properties based on extensive laboratory investigations (e.g., Ibsen and Bødker 1994; Ibsen et al. 2009). Typical index properties of this sand are shown in Table 1.

The soil was saturated using a similar procedure as reported by de Brum Passini and Schnaid (2015). An upward water flow from the perforated tube at the base of the model tank (Figs. 2*b* and 4*a*) with a hydraulic gradient lower than critical was applied. Since the saturation was carried out with water directly from the tap (oxygen rich) and special measures like adding backpressures or using CO_2 gas were not taken, a fully saturated soil model was not achieved. After saturation, the water level was kept constant at approximately 30 mm above the soil surface throughout the tests by using a weir at the top of the tank (Fig. 2*b*).

For each test, a model preparation technique following Foglia and Ibsen (2014) was adopted. This systematic approach enabled reuse of the initial soil model without emptying the model tank. The following procedure was used for each water flushing test:

1. *Sand loosening* (*approximately 15 min*) — Apply an upward water flow from the bottom of the tank through the perforated pipe using a hydraulic gradient close to critical.
2. *Pile positioning* — Position the pile vertically and horizontally above the soil surface using the pile template (Fig. 2). Fill the annulus between the casing and middle tube with water up to the backflow holes at the top of the pile while the packer remains closed.
3. *Pile pre-installation* — Penetrate the pile until it reaches its start position approximately 200 mm below the soil surface (Fig. 2) with limited water flow and no rotation. Open the packer to ensure that the water level inside the pile equalized to water level in the model tank. Close the packer.
4. *Sand compaction* — Densify the sand using a concrete vibrator by following a specified pattern (Fig. 5). The concrete vibrator was gently pushed down vertically until a defined penetration depth of approximately 600 mm was reached before it was slowly pulled up. Open the packer.
5. *Uniformity testing* — Test the uniformity of the sand model using a miniature cone. Figure 6 depicts the positions of these cone resistance tests.
6. *Pile drilling* — First, the data acquisition was switched on. Then, the flushing was turned on by opening the flow meter to a predefined value. Five seconds later, the pile rotation and penetration were turned on simultaneously. When the pile reached the end position of approximately 460 to 470 mm soil depth, penetration, rotation, and flushing was stopped at the same time and the packer was closed immediately to prevent sand particles flowing out of the pile casing.
7. *Cone resistance testing* — Cone resistance tests were carried out to investigate the influence from pile drilling.
8. *Pile lifting and collection of drill cuttings* — The pile was lifted and drill cuttings in the catch-pot and inside the pile were collected, dried, and weighed.

After the initial soil model preparation (Fig. 4), the sand was very loose with a mean relative density, D_r, of about 0.2. The relative density increased gradually after several rounds of loosening and compaction, reaching values between 0.6–0.65 for the presented tests. The mean relative density was calculated before each test based on the known total dry weight (m_s) and volume (v_s) of the sand in the model tank according to the following equations:

$$\rho_d = \frac{m_s}{v_s} \quad (1)$$

$$e = \left(\frac{\rho_s}{\rho_d}\right) - 1 \quad (2)$$

$$D_r = \frac{(e_{max} - e)}{(e_{max} - e_{min})} \quad (3)$$

Fig. 4. Stages in initial soil model preparation: (*a*) support for pore pressure standpipes and perforated tubes for saturation and drainage of soil model; (*b*) filter layer (LECA and geotextile); (*c*) geotextile as separation layer; (*d*) filling of dry sand. [Colour online.]

Table 1. Index properties of Baskarp sand No. 15 (after Ibsen and Bødker 1994).

Property	Value
D_{50} grain size (mm)	0.14
D_{60}/D_{10}	1.78
Grain density, ρ_s (g/cm^3)	2.64
Maximum void ratio, e_{max}	0.858
Minimum void ratio, e_{min}	0.549

Fig. 5. Grid for compaction of sand with concrete vibrator. Points "A" followed by points "B". (All dimensions in millimetres.)

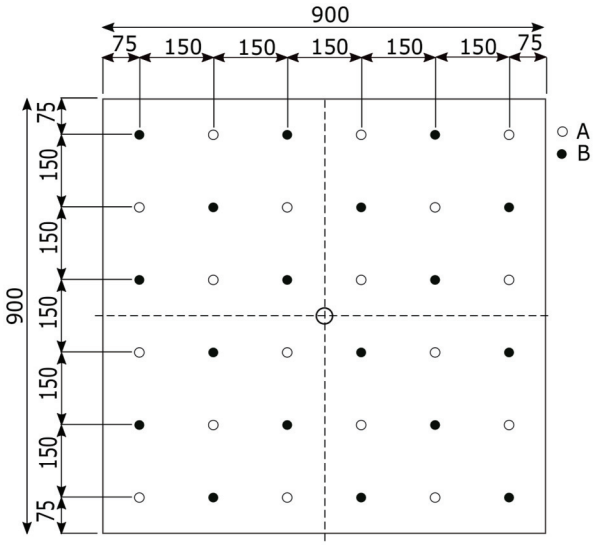

Fig. 6. Layout for cone resistance testing of sand model. Black dots represent positions for testing and r radial distance from pile centre. (All dimensions in millimetres.)

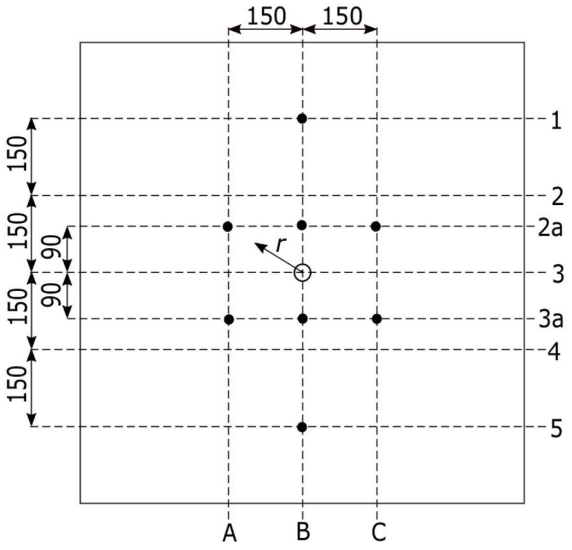

Cone resistance tests were carried out before the pile drilling to verify a consistent sand model preparation. A miniature cone with a diameter of 10 mm and an apex angle of 60° was connected to a steel rod and pushed 500 mm into the sand model using an actuator. The penetration rate used was 5 mm/s. Cone resistance tests were generally carried out after each soil model preparation and pile drilling test at distances of 90, 175, and 300 mm from the

Fig. 7. Cone resistance prior to pile drilling against depth measured at different radial distances from pile centre, *r*. [Colour online.]

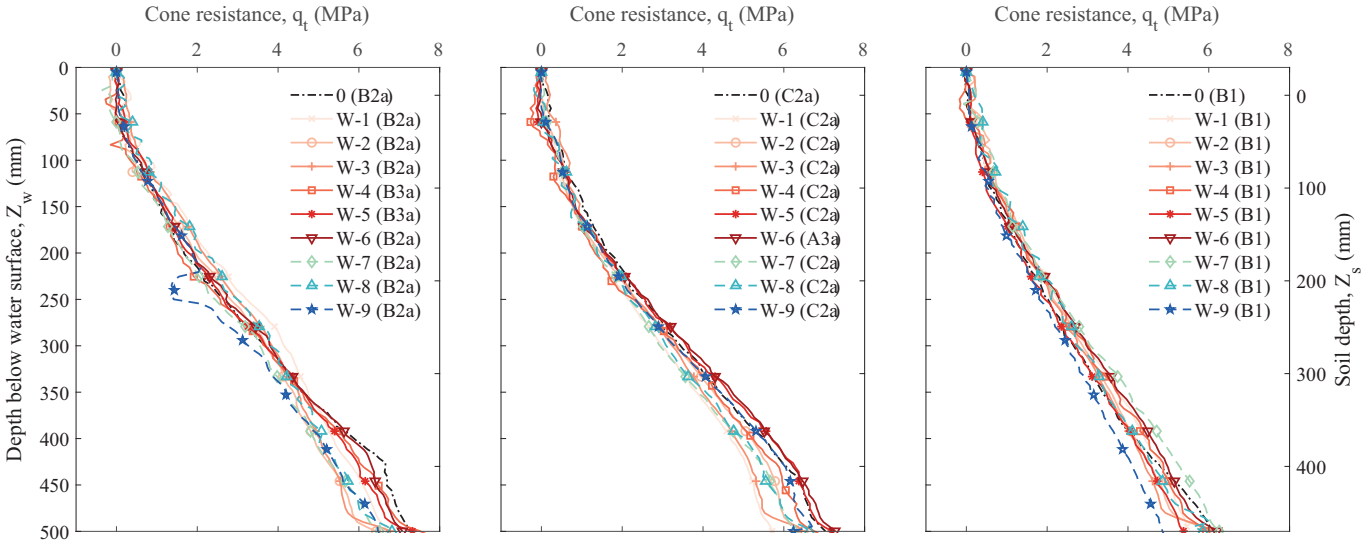

(a) r = 90 mm (b) r = 150 - 175 mm (c) r = 300 mm

Table 2. Test program.

Test No.	Flow rate (L/min)	Pressure (kPa)[a]	Penetration rate (mm/s)
0	—	—	2.5[b]
W-1	1.5	—	2.5[b]
W-2	2.0	—	2.5
W-3	2.5	—	2.5
W-4	3.0	15	2.5
W-5	4.0	35	2.5
W-6	5.0	60	2.5
W-7	2.0	—	2.0
W-8	2.0	—	3.0
W-9	2.0	—	4.0[b]
A-1	—	50	1.5
A-2	—	75	1.5
A-3	—	100	1.5

[a]Water pressure not measured for tests with flow rate below 3 L/min.
[b]A notable reduction of initial penetration rate of 2.5 mm/s was observed throughout the test.

Fig. 8. Load cell measurements against drilling depth. [Colour online.]

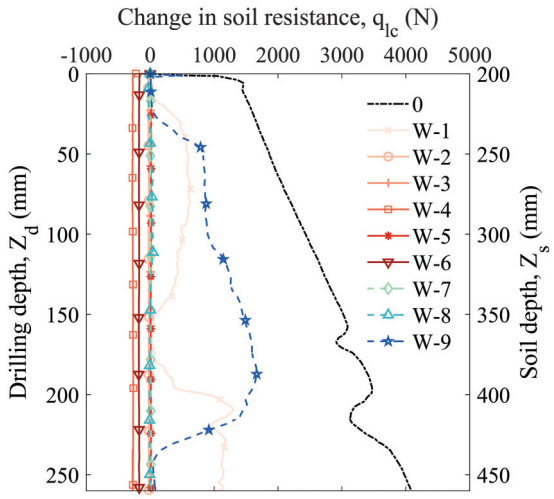

pile centre to assess the influence from drilling (Fig. 6). The order for testing in given positions were swapped for some of the pile tests to investigate potential local differences after the vibro-compaction.

Figure 7 shows measured cone resistance after vibro-compaction at different distances from the pile centre (*r*) against penetration depth. The results show a relatively high tip resistance at more than 200 mm soil depths, confirming that the compaction had a satisfying effect. The results also confirm a relatively uniform soil model. The data, however, reveal that the soil resistance at distance r = 300 mm (Fig. 7*c*) is slightly lower than at r = 90 mm (Fig. 7*a*) and r = 175 mm (Fig. 7*b*). This could likely be explained due to the vicinity to the model boundary. This trend was found to be consistent for the entire test series and considered to have a marginal impact on the test results. For test W-9, a reduced cone resistance was measured at a depth of approximately 220 mm below the soil surface (Fig. 7*a*). This irregularity was caused by hitting the catch-pot on the model pile during penetration and does not represent the real soil response.

2.4. Test procedure

An overview of the test program for this study is given in Table 2. The prefixes "W" or "A" indicate water or air flushing, respectively. Test 0 was carried out as a reference test by pushing the pile into the sand without any rotation and flushing. The flushing flow rate, Q, was varied between 1.5 to 5.0 L/min for the tests W-1 to W-6, while the penetration rate, V_{pen}, was kept constant at 2.5 mm/s. For the tests W-7 to W-9, the penetration rate varied between 2.0 and 4.0 mm/s while the flow rate was kept constant at 2.0 L/min. The starting value for the pile rotation was kept constant at 20 rpm for all tests except test 0. The flushing water pressure changed according to the given flow rate.

The tests A-1 to A-3 were carried out with the pile tip pre-installed to a starting depth of 400 mm and with flushing pressures of 50, 75, and 100 kPa, respectively. An increased starting depth compared to the water flushing tests was required, because initial tests at a starting depth of 200 mm (i.e., identical to the water flushing tests) caused immediate piping effects on the outside of the pile and drill cutting transport was not observed.

Fig. 9. Measured pore-water pressure changes against pile drilling depth in PP1 to PP6. [Colour online.]

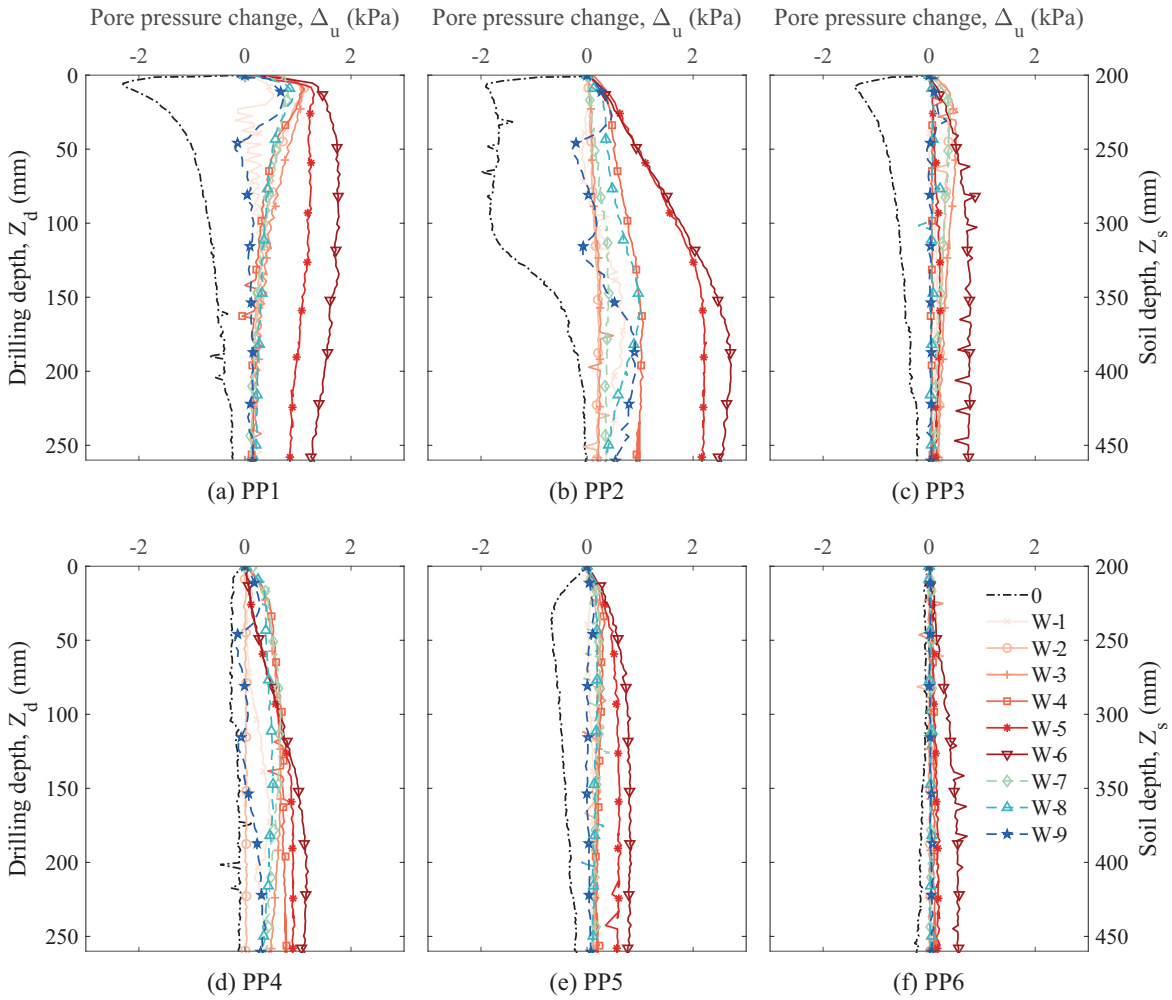

3. Water flushing tests

3.1. Influence on penetration resistance

Figure 8 shows the load cell measurements that provide a qualitative measure of the soil resistance against drilling depth. The start of drilling is at 200 mm soil depth (Figs. 2*b* and 2*c*). Test 0 (reference test) showed an immediate load increase to approximately 1400 N. This resistance aligns well with the expected bearing capacity of the pile tip at 200 mm soil depth. Further measurements show an almost linear increase in penetration force with depth, resulting in a maximum value of approximately 4100 N at a drilling depth of about 260 mm (soil depth Z_s = 460 mm). This equals a tip resistance of approximately 4.3 MPa, which is in the same range as the cone resistance tests (Fig. 7). Small decreases in load were observed at about 160 and 220 mm drilling depths. These differences—deviations from the linear trend could be explained by local inhomogeneities in the sand model.

Results from the water flushing tests W-2 to W-8 show no load or negative load values indicating tension caused by the self-weight of the model pile and rotation motor. The value of about –150 N matches the self-weight. This behaviour indicates that the soil did not provide any resistance, which is likely explained by local fluidization of the sand in front of the pile tip due to water flushing. Similar observations for pile jetting tests were reported by Tsinker (1988) and Shepley and Bolton (2014).

The load cell data for the tests W-1 and W-9 indicate that the flow rate (Q = 1.5 and 2.0 L/min, respectively) was too low to cause consistent local fluidization combined with the given initial penetration rate (V = 2.5 and 4.0 mm/s, respectively). For this reason, some soil resistance remained during drilling. This resulted in an increased penetration load compared to the other tests with maximum values of 1275 and 1665 N in tests W-1 and W-9, respectively. A reduction of the initial rotation speed was observed for these tests, which can be explained by substantial friction in the soil–pile interface. The results imply that both flow rate and penetration rate impact the soil behaviour surrounding the pile, and that these two parameters should be considered in combination when studying overburden drilling. A thorough discussion of these two parameters on the performance and effects on overburden will be presented below (Section 3.5).

3.2. Influence on pore-water pressure

Figure 9 presents the measured pore-water pressure changes (Δu) against pile drilling depth for the entire pore pressure sensors (PP1 to PP6) for test 0 (reference) and all the water flushing tests. Test 0 clearly stands out compared to the other tests. The data show a significant decrease in pore pressure as the pile was pushed into the sand; a maximum change of about –2.3 kPa in PP1 (Fig. 9*a*) occurred rapidly after the pile penetration started. The pore pressure slowly increased during penetration, being about 0.5 kPa lower than the initial starting value at the end of

Fig. 10. Normalized change in pore pressure against normalized distance from pile. Maximum pore pressure changes for (*a*) top PPs and (*b*) base PPs. Minimum changes in pore pressure for (*c*) top PPs and (*d*) base PPs. [Colour online.]

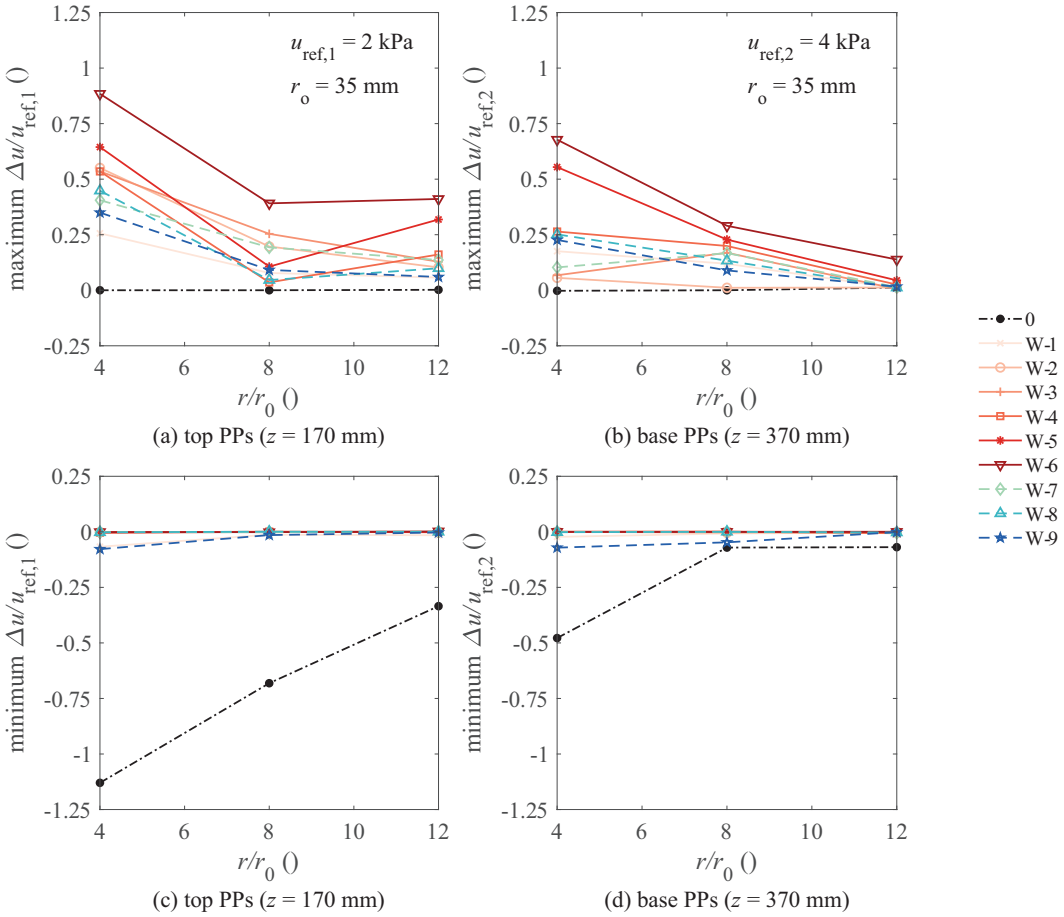

installation. Similar trends were also observed in PP3 (Fig. 9*c*) and PP5 (Fig. 9*e*); however, the influence decreased at greater distance from the pile. PP2 (Fig. 9*b*) showed an immediate pressure drop of about –1.9 kPa, but unlike the "top PPs" (PP1, PP3, PP5) the pressure did not increase again before the pile tip reached a soil depth of about 320 mm. This response may be explained by the pile moving closer to the "base PPs" while the distance to the top PPs increased. Only minor pressure reductions of about 0.2 kPa were measured in PP4 (Fig. 9*d*) and PP6 (Fig. 9*f*). The pressure reductions observed in test 0 are likely explained by dilation effects in the sand surrounding the pile tip and shaft like the behaviour of a driven closed-ended pile (e.g., White and Bolton 2004). When the relatively dense sand is displaced by the penetrating pile, large shear strains develop and cause a volume expansion (i.e., dilation). The soil becomes looser and pore water flows into the voids causing a pore pressure reduction.

All the water flushing tests (W-1 to W-9) caused excess pore pressures in the surrounding sand. The pore pressure changes are very moderate if compared to the applied input drilling fluid pressure up to about 60 kPa for test W-6. This indicates that most of the pressure is likely lost in the flushing tube, the drill bit, and the soil immediately surrounding the pile tip. As expected, the pore pressure values increase with the flow rate. Test W-1 (Q = 1.5 L/min) caused maximum pressure changes of about 0.5 kPa in PP1 and PP2 while test W-6 (Q = 5 L/min) showed corresponding values of about 1.7 and 2.8 kPa, respectively. Tests W-1 and W-9 were the only tests that caused some minor pressure reductions, i.e., negative pressure changes. This behaviour is likely explained by the same dilation effects as observed with test 0, which agrees with the results from the load cell measurements (Fig. 8).

PP1 at only 70 mm distance from the pile centre typically showed an immediate excess pressure when the flushing was turned on, before slowly dissipating again as the penetration depth increased. The base PPs installed at 370 mm soil depth (PP2, PP4, and PP6) displayed a more delayed response in excess pressures compared to the top PPs at 170 mm soil depth. This was expected as the base PPs where furthest from the pile tip at the beginning of the tests; hence, the maximum influence was recorded when the pile tip reached approximately the same depth as the base PPs (i.e., a drilling depth of approximately 200 mm). PP5 and PP6 at a horizontal distance of approximately 210 mm from the pile centre generally showed minor pressure changes during the tests. Only for test W-6, approximately 0.5 to 0.7 kPa excess pressure was measured by PP5 and PP6. For the tests with varying penetration rates (i.e., W-7 to W-9), clear trends in pore-water pressure changes were not observed.

Figure 10 shows the ratio between the pore pressure change (Δu) and the reference pressure (u_{ref}) against the normalized radial distance from the pile (r/r_0), where r_0 is the pile radius and r the radial distance from the pile. Figures 10*a* and 10*b* present the maximum pore pressure change (Δu_{max}) for the top PPs and base PPs, respectively, while Figs. 10*c* and 10*d* present the minimum pore pressure change (Δu_{min}). The reference pressure is defined as the hydrostatic head at the theoretical position of the standpipe ends (i.e., filter positions) that results in a pore-water pressure of 2 kPa for the top PPs and 4 kPa for the base PPs. From Fig. 10 the

Fig. 11. Soil surface settlements against drilling depth for (*a*) LVDT1, (*b*) LVDT2, (*c*) LVDT3, and (*d*) LVDT4. Negative values indicate settlements. [Colour online.]

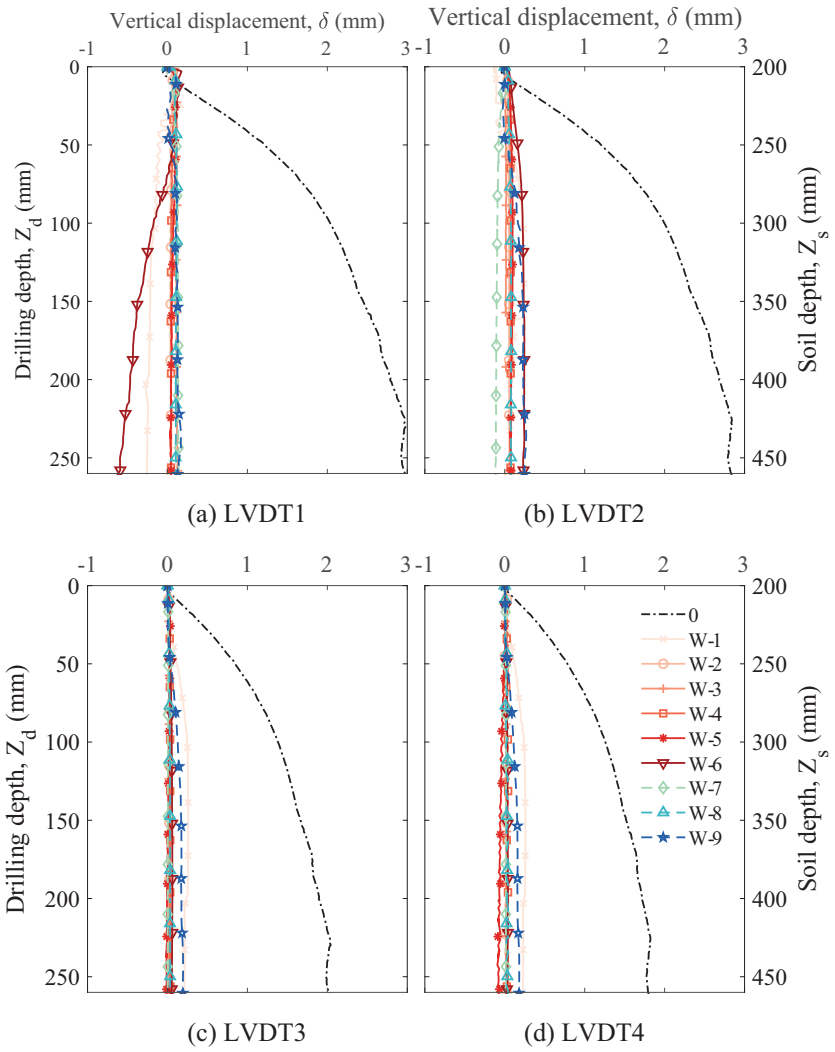

pore pressure change generally decreases with distance from the pile. This trend is more prominent for the tests with considerable flow rates (i.e., W-5 and W-6) and for the base PPs at 370 mm soil depth (PP2, PP4, and PP6). The data further indicate that the normalized change in pore pressure is less in the base PPs compared to the top PPs. This can be explained by the increase of the reference pressure with depth.

3.3. Influence on soil displacements

Figure 11 presents the measured vertical soil displacement (δ) against drilling depth for the four LVDTs. For test 0, a significant soil heave was monitored. This effect was expected because the pile was pushed in like a closed-ended displacement pile. However, LVDT1 and LVDT2 both show a small (approx. 0.1 mm) settlement before the heave begins after 5 to 10 mm penetration. This behaviour is likely explained by a combination of the penetrating pile and the loose state of the soil close to the surface. The initial pile penetration caused a compaction of the top soil adjacent to the pile before dilation effects became dominant and heave occurred. LVDT1 positioned 35 mm from the pile centre showed a maximum heave of approximately 3 mm (Fig. 11*a*), which reduced to 1.8 mm in LVDT4 at about 210 mm distance from the pile centre (Fig. 11*d*).

Results from the water flushing tests generally showed small soil surface displacements. Test W-1 indicates some minor heave (0.1–0.2 mm) in all LVDTs except LVDT1 closest to the pile that settled at about 0.3 mm. Test W-9 caused heave in all the LVDTs. The heave in tests W-1 and W-9 could be explained by the pile drilling causing some soil displacements as the flushing was only able to partially fluidize and remove the sand in front of the drill bit (see above).

Visual observations after drilling showed that all water flushing tests as well as test 0 caused a small cavity (recess) in the soil surface with about 10 mm influence from the pile casing. Figure 12 shows a photo of such a cavity after the completion of test W-4. This effect could not be captured by LVDT1 due to its too large distance of about 17.5 mm from the pile casing. The size of this cavity remained almost constant for the conducted tests, thus being independent of the flushing flow rate and penetration rate. The cavities most likely occurred because at very shallow depths the failure mechanism does not present any dilative behaviour and so, for the first centimetres of penetration, the soil adjacent to the pile tends to densify. The cone penetration tests confirm this hypothesis showing very low resistance in the first 100 mm of penetration and a similar cavity. A supplementary test that is not reported in this paper was carried out with the same flow and

Fig. 12. Local cavity at soil surface around pile casing after test W-4. [Colour online.]

penetration rate as test W-2, but without pile rotation. This test resulted in a noticeable smaller cavity, which may indicate that the pile rotation even further increased this densification adjacent to the casing.

Given that the flow rate in test W-1 was not able to fluidize the sand completely, some of the soil resistance remained (Fig. 8). The penetrating pile caused less compaction effects as observed in test 0. Some drill cutting transport through the pile occurred, which likely reduced dilation effects and probably contributed to the settlements measured in LVDT1 of test W-1. Test W-6 resulted in about 0.6 mm settlement in LVDT1, but no significant displacement in the other LVDTs. These settlements are likely due to the high flow rate causing considerable erosion and loss of soil volume around the pile, which is further discussed below. The other water flushing tests showed negligible soil surface displacements.

3.4. Influence on soil resistance

Cone resistance tests after each pile drilling test were used to assess the impact of different drilling parameters on the soil. Figure 13 presents the measured cone resistance at different distances from the pile centre (r) against penetration depth for test 0 and the water flushing tests. The results for a distance r of 90 mm indicate a general trend of reduced cone resistance with increasing flow rate (Fig. 13*a*). This difference is particularly noticeable between the tests W-4 to W-6. For the tests W-1 to W-4, this trend is less obvious, which most likely is explained by the relatively small variations in flow rates. Test W-6 clearly stands out compared to the other water flushing tests with a significant lower soil resistance from about 200 mm soil depth until the final depth of about 480 mm. The results show an unexpected lower soil resistance after test W-9 compared to test W-8 even though the penetration rate was higher. Based on the load cell measurements (Fig. 8) it is likely that the high penetration rate (5 mm/s) with test W-9 caused soil displacements and dilation effects that reduced the soil resistance. The same effect could also explain why test W-1 shows less resistance than observed after the tests W-2, W-3, and W-8.

Figure 13*b* shows cone resistance from the positions with a distance between 150 to 175 mm from the pile centre excluding data for the tests W-2, W-3, and W-9. Due to the greater distance to the pile, the trends observed above diminish. The results do not show an influence from any of the tests at a distance of r = 300 mm (Fig. 13*c*).

An interesting observation is that test 0 caused the lowest cone resistance in the surrounding sand for all tests. The considerable installation effect is clearly visible at both 90 (Fig. 13*a*) and 175 mm (Fig. 13*b*) distance from the pile while the impact diminished at a radial distance of 300 mm (Fig. 13*c*). A possible explanation could be that the soil displacements due to the pile penetration without flushing caused large shear strains and volumetric expansion that reduced the soil resistance. This behaviour agrees with results from pile tests in sand (White and Bolton 2004) and triaxial tests on Baskarp sand No. 15 showing large dilation angles up to 18° for low stress conditions (Ibsen et al. 2009). This finding is in accord with results from LVDTs and is to some degree also applicable for the tests W-9 and W-1.

Figure 14 shows the cone resistance at different radial distance from the pile centre before ("pre") and after ("post") the tests W-6 (Fig. 14*a*) and 0 (Fig. 14*b*). As discussed above, test W-6 shows that at r = 90 mm the soil resistance reduced considerably after the pile drilling (B2a versus B3a, Fig. 14*a*) with a maximum difference of approximately 3.2 MPa at about 400 mm soil depth. The results show a notable influence also at 175 mm from the pile (A3a versus C2a, Fig. 14*a*) with a maximum reduction in the cone resistance of about 1.1 MPa. For r = 300 mm the difference between pre- and post-test resistance appears to be negligible (B5 versus B1, Fig. 14*a*). Test 0 shows a similar behaviour. However, a greater reduction in the soil resistance due to the pile test can also be seen at r = 175 mm (A2a versus C2a, Fig. 14*b*). This implies that the radial influence was greater for test 0.

3.5. Effect of flushing parameters on drill cuttings transport

An important aspect to understand the mechanism of overburden drilling is to assess the balance between the generated drill cuttings and the theoretically replaced soil mass represented by the pile volume generated during drilling (i.e., installed pile volume). For this reason, the mass of drill cuttings, M_c, which is the sum of the soil collected in the catch-pot and in the annulus between the casing and the middle tube of the model pile, was measured for each test. The obtained data indicates that the variations of the flushing parameters considerably affected the mass of drill cuttings. To highlight this finding, non-dimensional parameters of normalized flow, Q_{norm}, and normalized mass of drill cuttings, $M_{c,norm}$, were introduced. The normalized flow is defined as:

$$Q_{norm} = \frac{Q}{A_{pile} V_{pen}} \quad (4)$$

where Q is the flushing flow rate in dm^3/min, A_{pile} is the cross-sectional area of the pile in dm^2, and V_{pen} is the penetration rate in dm/min. This dimensionless parameter combines both the flow and penetration rate with the pile area, and therefore provides a simple means to evaluate the effect of flushing parameters on the drill cuttings transport.

The normalized mass of drill cuttings, $M_{c,norm}$, is defined as the ratio between the mass of drill cuttings, M_c, collected from the pile throughout a test and the theoretical mass of soil, M_{pile}, given by the installed pile volume and the calculated relative density of the respective soil model. This calculation disregards potential drilling induced soil displacements and soil volume changes, which is a simplification. A value lower than 1 indicates that the mass of drill cuttings is less than the theoretical one,

Fig. 13. Cone resistance against depth for test 0 and tests W-1 to W-9 at radial distance from pile centre of: (*a*) 90 mm; (*b*) 175 mm; (*c*) 300 mm. [Colour online.]

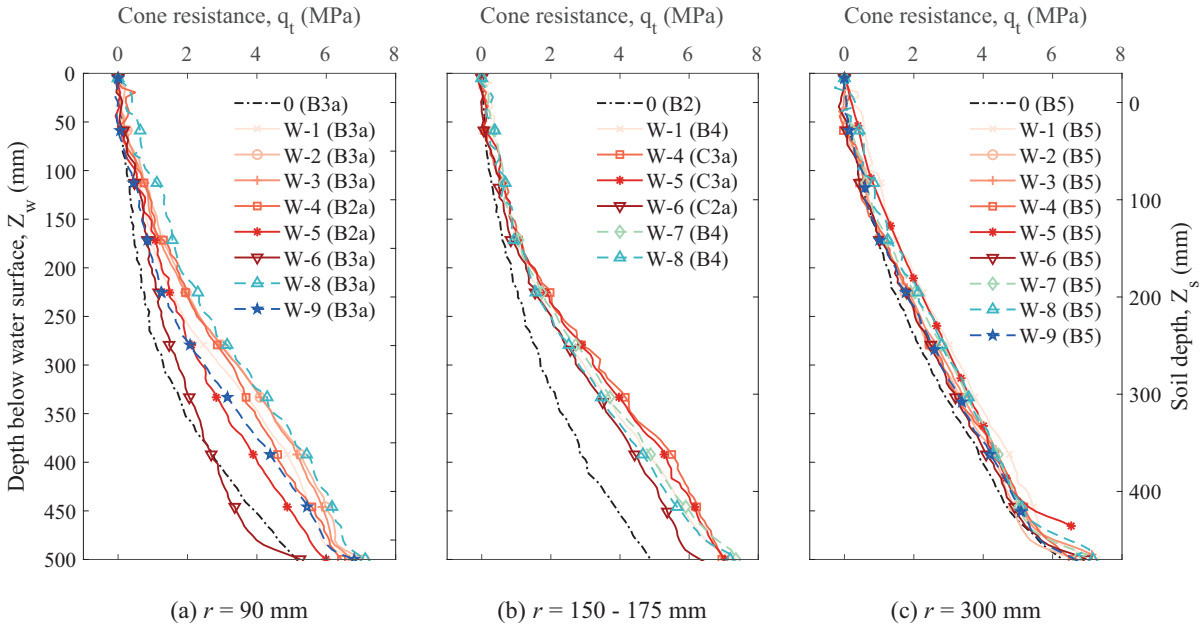

Fig. 14. Comparison of cone resistance against depth at different radial distances (*r*) from pile centre prior to ("pre") and after ("post"): (*a*) test W-6 and (*b*) test 0. [Colour online.]

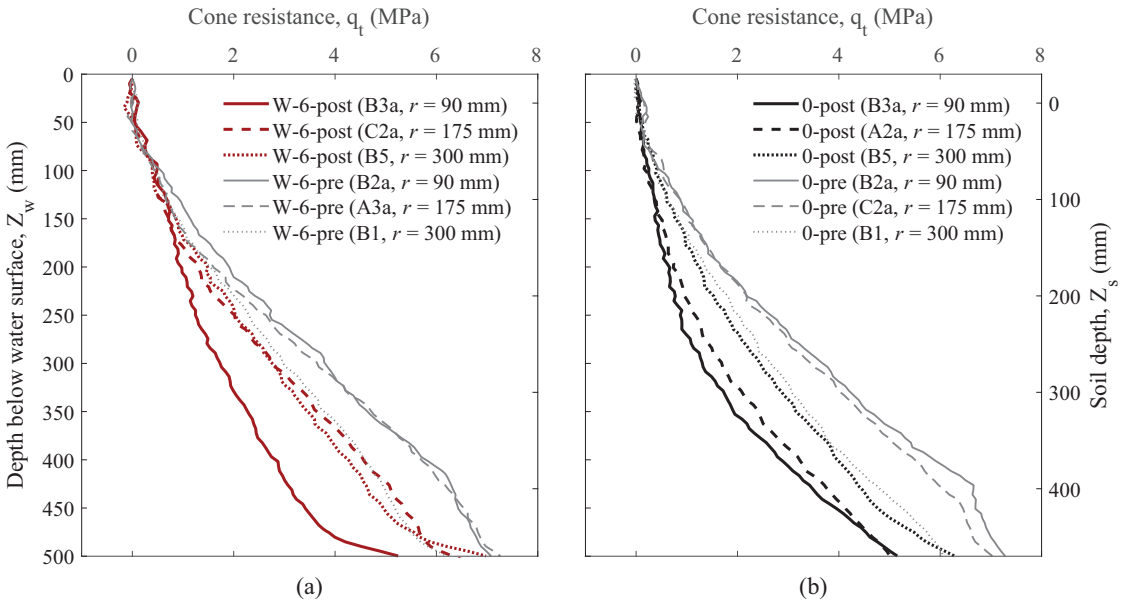

meaning that the soil is likely replaced by the pile drilling. A value above 1 indicates that the mass of drill cuttings is higher than the theoretical mass, hence causing a potential soil volume loss. A value of 1 is defined as an "ideal" scenario.

Figure 15 presents normalized flow rate, Q_{norm}, against normalized mass of drill cuttings, $M_{c,norm}$ (Fig. 15*a*) and the maximum change in soil resistance, q_{lc}, measured by the load cell (Fig. 15*b*). The results show an overall linear trend of increase in normalized mass of drill cuttings with normalized flow rate. The data reveal that an increase in the flow rate caused an increase in the normalized mass of drill cuttings (compare tests W-1 to W-6). By contrast, an increase of the penetration rate reduced the mass of drill cuttings (compare test W-2 and tests W-7 to W-9). This indicates an inverse correlation between the parameters flow rate and penetration rate.

Given that test 0 was carried out without flushing, the normalized flow and the mass of drill cuttings were zero. The tests W-1 and W-9 both resulted in a value for $M_{c,norm}$ of about 0.85 with a corresponding value of Q_{norm} just below 10. This indicates that the installation caused some soil displacement surrounding the pile, which is supported by the observed increase in penetration resistance in parts of these tests as can be seen in Fig. 15*b* (and Fig. 8). For test W-1 the penetration rate of 2.5 mm/s means that a soil volume of approximately 0.14 L/min should be displaced by the pile

Fig. 15. Normalized flow rate (Q_{norm}) against (*a*) normalized mass of drill cuttings ($M_{c,norm}$) and (*b*) maximum change in soil resistance, q_{1c}, measured by load cell. [Colour online.]

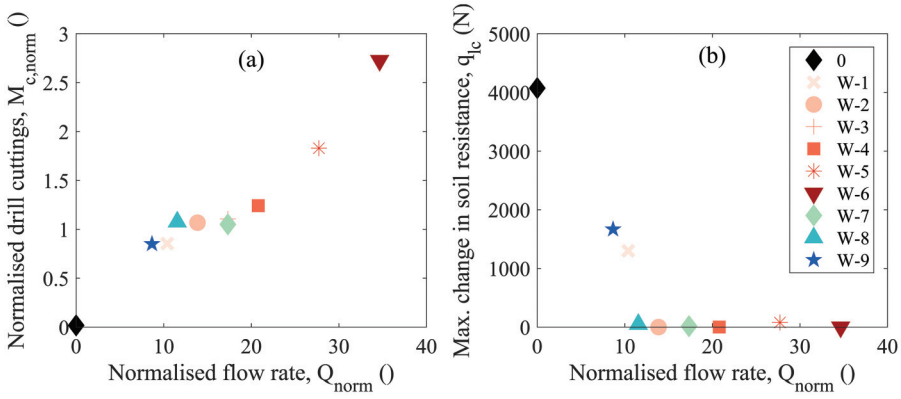

tip, i.e., removed by drilling. The flow rate was about 10 times higher (Q = 1.5 L/min), which is similar in value to that of test W-9. This indicates that the flow rate needs to be large enough to be able to attain a specific penetration rate, or alternatively the penetration rate needs to be adapted to the flow rate.

Test W-2 (Q = 2.0 L/min) represents an almost ideal scenario for the modelled conditions with $M_{c,norm}$ of about 1.07, only about 7% excess drill cuttings compared to the installed pile volume was measured. This is in line with the small load cell and pore-water pressure readings observed for this test (Fig. 15*b* and Fig. 9). A maximum $M_{c,norm}$ and Q_{norm} value of about 2.7 and 35, respectively, was obtained for the test W-6 (Q = 5.0 L/min). This significant loss of soil volume likely explains the settlements observed with LVDT1 (Fig. 11*a*). However, the other LVDTs at greater distance from the pile showed minor settlements. This observation might be related to soil loosening (i.e., reduction in relative density) caused by the high flow rate, which likely compensates the soil volume loss adjacent to the pile. The significant reduction in cone resistance measured after the test (Fig. 14*a*) supports this interpretation. At prototype stress conditions it is likely that the extensive loss of soil volume observed for test W-6 would lead to considerable ground settlements.

The experimental data reveal that a normalized flow rate between 10 to 20 results in an "ideal drilling" in terms of drill cuttings balance, i.e., $M_{c,norm}$ equal or close to 1.0. Compared to prototype drilling in medium dense sand with a casing diameter of 76 mm, typical values for normalized flow rate are estimated to vary from about 20 to 55 with a given flow rate, Q, from 80 to 150 L/min and an assumed penetration rate, V_{pen}, from 500 to 1000 mm/min (8.33 to 16.66 mm/s). These values are higher than the obtained "ideal" normalized flow rate and according to Fig. 15*a* would result in a too high drill cutting transport. The difference is likely a result of the low stress conditions modelled, and refined investigations are required to translate this framework into practice.

3.6. Air flushing tests

Tests carried out with air flushing were generally not able to create a successful transport of drill cuttings. An increased starting soil depth of 400 mm improved the flushing backflow. At the beginning of the tests A-1 to A-3 small outbursts of water, sand, and air were observed at the pile top. However, after about 15 to 20 s of drilling the air caused soil fractures and piping (i.e., flow paths) along the outside of the pile wall, which continued until the tests were stopped after 100 mm of drilling. This effect has been observed in the field when drilling with air flushing is carried out at shallow depths or when the flushing pressure is too high (e.g., Lande et al. 2020; Sandene et al. 2021). Due to these challenges the air flushing tests could not be compared with the water flushing tests.

Figure 16 presents pore-water pressure changes (Δu) against pile drilling depth for the tests A1 to A3. The results generally display a reduced pore pressure in the surrounding ground, which could indicate that the air flushing caused an air-lift pump effect as suggested in case studies (Lande et al. 2020; Ahlund and Ögren 2016; Bredenberg et al. 2014). However, the limited dataset makes the analysis challenging and no clear conclusions can be drawn. As seen in the Figs. 16*a*, 16*c*, and 16*e* only minor changes were observed in the top PPs (PP1, PP3, and PP5). This is likely explained by the starting depth of 400 mm and the distance from the pile tip to these top PPs. PP2 (Fig. 16*b*) and PP4 (Fig. 16*d*) at 370 mm soil depth experienced the largest pore pressure reductions with maximum values of about –0.6 kPa for test A-1 and A-2, respectively. Despite the highest flushing pressure (i.e., 100 kPa), test A-3 caused less influence compared to the other tests.

Results from the load cell measurements presented in Fig. 17 suggest that the air flushing was not able to fluidize and loosen the sand as the water flushing did (Fig. 8). In general, an increase in penetration force with depth was observed until the drilling stopped. Only test A-2 showed a reduced resistance from about 45 to 85 mm drilling depth until it increased again. The tests A-1 and A-3 reached a maximum value of approximately 3600 N and test A-2 a value of 2300 N. Given that the load cell data display similar trends and penetration force as with test 0, the pore pressure reductions might be related to dilation effects.

Data from the load cell and the observed lack of drill cuttings transport give reason to assume that the air flushing pressure and flow rate was too low to remove the drill cuttings in front of the drill bit during drilling. Due to the low effective soil stresses sudden piping was observed, and the air pressure could not be further increased. However, after the tests some sand sticking to the inside of the pile casing was detected.

4. Applicability of results

Overburden drilling is characterized by very complex simultaneous processes that are carried out in varying ground conditions. For that reason, some simplifications were necessary in the described experiments. The test set-up did not replicate the details of a percussive hammer that is typically used in overburden drilling to maintain an acceptable penetration rate when drilling in dense granular soils and rock (Sabatini et al. 2005; Finnish Road Authorities 2003). The effect of this parameter on the surrounding ground is likely insignificant for the modelled ground conditions. All tests were carried out under 1g conditions at rather low soil stresses, thus having some unavoidable limitations compared to prototype drilling in the field. Consequently,

Fig. 16. Measured pore-water pressure changes against pile drilling depth in PP1 to PP6 for air flushing tests. [Colour online.]

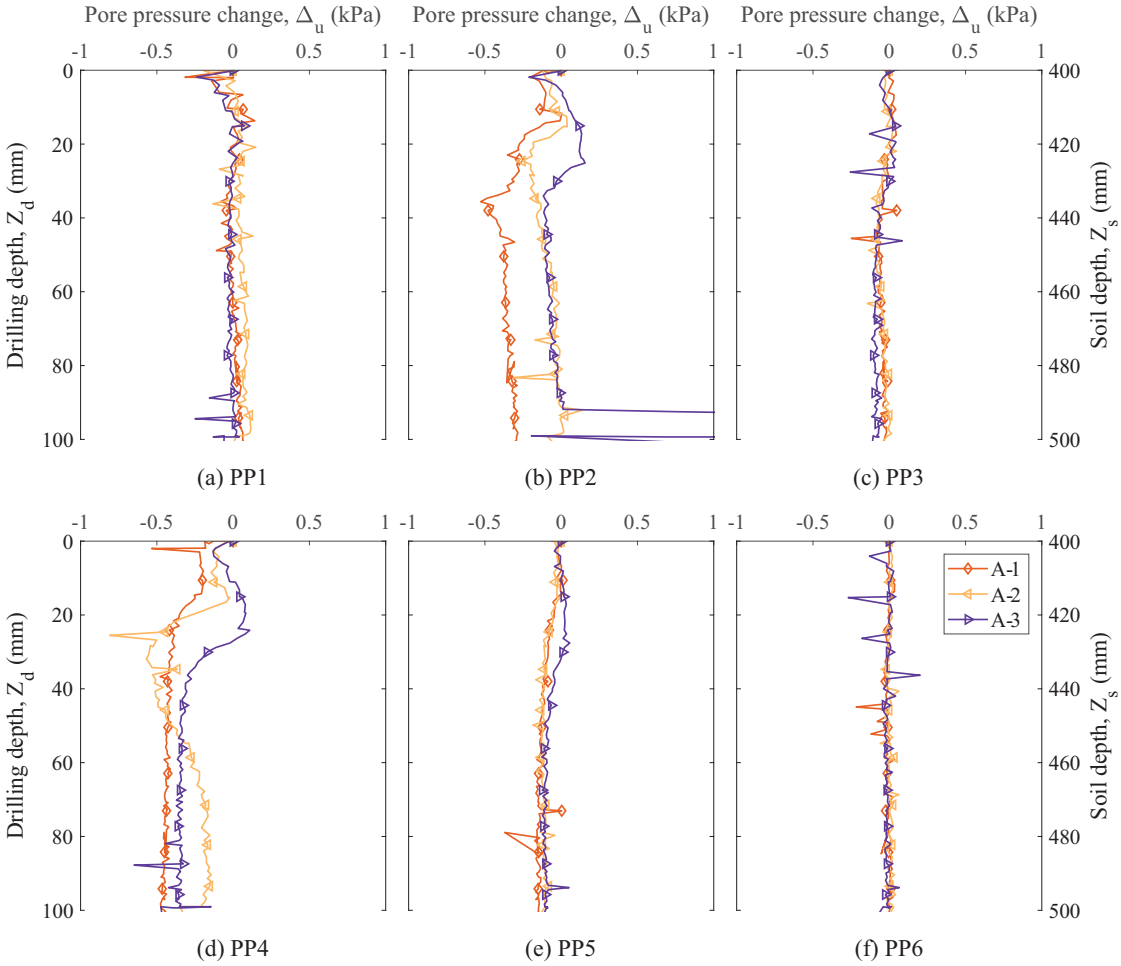

Fig. 17. Load cell measurements against drilling depth for air flushing tests. [Colour online.]

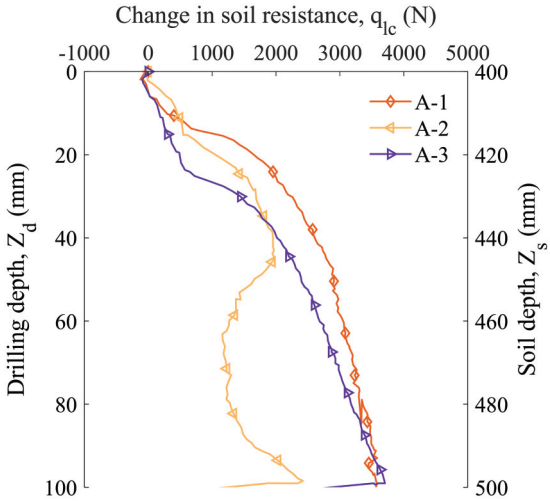

the flushing pressures and flow rates used in the tests were lower than in a real case scenario making it difficult to compare the normalized flow rate values from the tests directly with prototype drilling parameters. The limited soil depth and soil stress most likely affected the range of normalized flow rate at which an "ideal" drilling scenario was identified (Fig. 15*a*).

To further investigate the physical effects from drilling on the surrounding ground and to be able to reliably translate the obtained results into practice, refined model tests including more representative soil stresses, hydraulic conditions (e.g., confined aquifer), and flushing parameters are recommended. Future tests should include higher and more representative soil stresses (e.g., by adding a surcharge) and pore-water pressures representative for drilling at larger soil depth. Higher soil stress would likely require increased flushing parameters (i.e., flow rate and pressure). Other aspects that should be investigated are (*i*) the effect of drilling in a confined aquifer (e.g., under an impermeable soil layer) as frequently observed in the field (Lande et al. 2020; Ahlund and Ögren 2016; Sandene et al. 2021), (*ii*) the influence of varying soil density, (*iii*) different degrees of saturation, and (*iv*) the impact of different pile rotation rates.

It is expected that refined tests will provide further insight into overburden drilling. Such results in combination with the introduced framework of normalized drill cutting transport and flow rate could lead to practical recommendations regarding a more informed choice of overburden drilling systems and parameters.

The introduced framework should be investigated further through full-scale testing to validate its applicability.

5. Conclusions

This paper presents physical model tests to study the effects from overburden drilling of piles on the surrounding ground. Novel experimental data are provided that reveal the impact of different flushing media (i.e., water and air) and flushing parameters such as flow and penetration rate on the penetration force, pore pressure changes, soil displacements, and drill cuttings transport. Based on the results of the water flushing tests, the following conclusions can be drawn:

1. Increasing flow rates caused larger excess pore-water pressures with a greater influence area in the surrounding soil. The measured pore pressure changes were generally small and decreased with the distance from the pile. An increased flow rate generated more drill cuttings and reduced the soil resistance significantly in the soil adjacent to the pile.
2. An increased penetration rate compensated the effects observed when increasing the flow rate. This observation indicates an inverse correlation between these parameters.
3. The drill cutting transport depends on both the flow and penetration. The experimental results indicate an almost linear relationship between the normalized flow rate, Q_{norm}, which relates the flow to the penetration rate and the cross-sectional area of the model pile, and the normalized mass of drill cuttings, $M_{c,norm}$.
4. For high normalized flow rates, Q_{norm}, the soil in front of the drill bit fluidized, which reduced or practically eliminated the penetration resistance. This response is comparable to observations during pile jetting. The fluidization, however, may lead to considerable ground settlements. For the tests with too low flow rate (e.g., W-1) or too high penetration rate (e.g., W-9), opposite behaviour was observed, and the soil resistance partly remained.
5. The introduced framework of normalized flow rate, Q_{norm}, and normalized mass of drill cuttings, $M_{c,norm}$, could provide a first effective means to derive ideal drilling parameters. The experimental data reveal that a normalized flow rate between 10 to 20 results in an "ideal" drilling in terms of drill cuttings balance, i.e. $M_{c,norm}$ equal or close to 1.0. The effect of more representative soil stresses is, however, an area that requires further research.

The air flushing tests were limited by modelling constraints; thus, no clear conclusions can be drawn from these tests. However, a notable reduction of pore pressures adjacent to the casing was measured. This finding may indicate that air flushing causes a behaviour equivalent to an air-lift pump effect that could lead to considerable erosion, soil loss, and resulting ground movements. Similar observations were reported in case studies (Lande et al. 2020; Ahlund and Ögren 2016; Bredenberg et al. 2014).

The presented experimental data provide a new insight into the mechanisms of overburden drilling on the surrounding ground. Refined model tests that should focus on more representative stress conditions and flushing parameters are recommended. In addition, full-scale tests should be explored to further assess the introduced framework of normalized drill cutting transport and flow rate to evaluate the obtained data.

Acknowledgements

The authors would like to acknowledge The Research Council of Norway (RCN) and the 18 partners in the research project "BegrensSkade II – Risk reduction of Groundwork Damage" (RCN project No. 267674) for funding of the model tests. The authors would also specifically like to acknowledge NGI's staff: Axel Walta for the mechanical design of the model pile, Ole Petter Rotherud for help with setting up the data acquisition system, and the excellent staff at NGI's workshop for help with practical issues related to the model test.

References

Ahlund, R., and Ögren, O. 2016. Pore pressures and settlements generated from two different pile drilling methods. M.Sc. thesis, Department of Civil and Architectural Engineering, Royal Institute of Technology, KTH, Stockholm.

Alsaydalani, M.O.A., and Clayton, C.R.I. 2014. Internal fluidization in granular soils. Journal of Geotechnical and Environmental Engineering, ASCE, **140**(3): 04012024. doi:10.1061/(ASCE)GT.1943-5606.0001039.

Asplind, M. 2017. Pore-water pressure and settlements generated from water driven DTH-drilling. A field study. M.Sc. thesis, Department of Civil and Architectural Engineering, Royal Institute of Technology, KTH, Stockholm.

Behringer, H. 1930. Die Flüssigkeitsförderung nach dem Prinzip der Mammutpumpe [Pumping liquids according to the principle of the mammoth pump]. Doctoral dissertation, Technical University of Karlsruhe. [In German.]

Bredenberg, H., Jönsson, M., Isa, R., Larsson, M., and Larsson, E.L. 2014. Borrteknik för minimering av marksättninger vid borrad grundläggning [Drilling technique for minimizing ground settlements from drilling of foundation piles]. Bygg & Teknik 1/14. [In Swedish.]

de Brum Passini, L., and Schnaid, F. 2015. Experimental investigation of pile installation by vertical jet fluidization in sand. Journal of Offshore Mechanics and Arctic Engineering, **137**: 042002. doi:10.1115/1.4030707.

Epiroc. 2020. Rock drilling tools. Available from https://www.epiroc.com/en-hr/products/rock-drilling-tools [accessed 16 June 2020].

Finnish Road Authorities. 2003. Instructions for drilled piling: design and execution guide — Guidelines for design and implementation. Helsinki. ISBN 951-803-026-X.

Foglia, A., and Ibsen, L.B. 2014. Laboratory experiments of bucket foundations under cyclic loading. DCE Technical reports, No. 177. Department of Civil Engineering, Aalborg University, Aalborg.

Ibsen, L.B., and Bødker, L. 1994. Baskarp Sand No. 15. Data report No. 9401. Geotechnical Engineering Group, Aalborg University Centre, Aalborg, Denmark.

Ibsen, L.B., Hanson, M., Hjort, T., and Thaarup, M. 2009. MC-Parameter Calibration of Baskarp Sand No. 15. DCE Technical Reports, No. 62. Department of Civil Engineering, Aalborg University, Aalborg.

Karlsrud, K., and Andresen, L. 2008. Design and performance of deep excavations in soft clays. *In* Proceedings of the 6th International Conference on Case Histories in Geotechnical Engineering. Missouri University of Science and Technology, Arlington, Va.

Kato, H., Tamiya, S., and Miyazawa, T. 1975. A study of an air-lift pump for solid particles and its application to marine engineering. *In* Proceedings of the 2nd Symposium on Jet Pumps, Ejectors and Gas Lift Techniques. Churchill College, Cambridge, UK. pp. G3-37–G3-49.

Konstantakos, D.C., Whittle, A.J., Regalado, C., and Scharner, B. 2004. Control of ground movements for a multi-level-anchored, diaphragm wall during excavation. *In* Proceedings of the 5th International Conference on Case Histories in Geotechnical Engineering, New York. Paper No. 5.68.

Kullingsjø, A. 2007. Effects of deep excavations in soft clay on immediate surroundings – Analysis of the possibility to predict deformations and reactions against the retaining system. Doctoral thesis, Chalmers University of Technology, Gothenburg, Sweden. ISBN 978-91-7385-002-5.

Lande, E.J, Karlsrud, K., Langford, J., and Nordal, S. 2020. Effects of drilling for tieback anchors on surrounding ground — results from field tests. Journal of Geotechnical and Geoenvironmental Engineering, ASCE, **146**(8): 05020007. doi:10.1061/(ASCE)GT.1943-5606.0002274.

Langford, J., Karlsrud, K., Lande, E.J., Eknes, A.Ø., and Engen, A. 2015. Causes of unexpectedly large settlements due to deep excavations in clay. *In* Proceedings of the 16th European Conference on Soil Mechanics and Geotechnical Engineering, Edinburg, 13–17 September 2015. ICE Publishing, London, U.K. pp 1115–1120. doi:10.1680/ecsmge.60678.vol3.156.

Mana, A.I., and Clough, G.W. 1981. Prediction of movements for braced cuts in clays. Journal of the Geotechnical Engineering Division, **107**: 759–777.

Peck, R.B. 1969. Deep excavations and tunneling in soft ground. *In* Proceedings of the 7th International Conference on Soil Mechanics and Foundation Engineering, Mexico City. pp. 225–290.

Sabatini, P.J., Tanyua, T., Armour, T., Groneck, P., and Keeley, J. 2005. NHI Course No. 132078: Micropile design and construction — Reference manual. Publication No. FHWA NHI-05-039. National Highway Institution, Federal Highway Administration, U.S. Department of Transportation, Washington, D.C.

Sandene, T., Ritter, S., and Lande, E.J. 2021. A case study on the effects of anchor drilling in soft, low sensitive clay and sandy, silty soils. *In* Proceedings of the 10th International Symposium on Geotechnical Aspects of Underground Construction in Soft Ground, Robinson College, Cambridge, UK., 29–30 June 2021. Taylor and Francis Publishing.

Shepley, P., and Bolton, M.D. 2014. Using water injection to remove pile base resistance during installation. Canadian Geotechnical Journal, **51**(11): 1273–1283. doi:10.1139/cgj-2013-0240.

Tsinker, G.P. 1988. Pile Jetting. Journal of Geotechnical Engineering, ASCE, **114**(3): 326–334. doi:10.1061/(ASCE)0733-9410(1988)114:3(326).

van Zyl, J.E., Alsaydalani, M.O.A., Clayton, C.R.I., Bird, T., and Dennis, A. 2013. Soil fluidization outside leaks in water distribution pipes - Preliminary observations. Proceedings of the Institution of Civil Engineers - Water Management, **166**(10): 546–555. doi:10.1680/wama.11.00119.

White, D.J., and Bolton, M.D. 2004. Displacement and strain paths during plane-strain model pile installation in sand. Géotechnique, **54**(6): 375–397. doi:10.1680/geot.2004.54.6.375.

List of symbols

A_{pile}	cross-sectional area of pile (mm^2)
D_{10}	10% fractile in grain-size distribution (mm)
D_{50}	50% fractile in grain-size distribution (mm)
D_{60}	60% fractile in grain-size distribution (mm)
D_r	relative soil density
e	void ratio
e_{max}	maximum void ratio
e_{min}	minimum void ratio
M_c	measured mass of drill cuttings (g)
$M_{c,norm}$	normalized mass of drill cuttings
M_{pile}	theoretical mass of soil given by installed pile volume (g)
m_s	mass of dry sand in model tank (g)
Q	flushing flow rate (L/min)
Q_{norm}	normalized flow rate
q_{lc}	change in soil resistance (N)
q_t	cone resistance (MPa)
r	radial distance from pile centre (mm)
r_0	pile radius (mm)
u_{ref}	reference pore-water pressure (kPa)
Δu	change in pore-water pressure from reference value (kPa)
Δu_{max}	maximum pore pressure change (kPa)
Δu_{min}	minimum pore pressure change (kPa)
V_{pen}	drilling penetration rate (mm/s)
v_s	volume of dry sand in model tank (cm^3)
Z_d	drilling depth (mm)
Z_s	soil depth (mm)
Z_w	depth from water surface (mm)
δ	vertical displacement of soil surface (mm)
ρ_d	dry density (g/cm^3)
ρ_s	grain density (g/cm^3)
$\varnothing$	pile diameter